Research & Reviews: Journal of
Space Science & Technology
https://journals.stmjournals.com/rrjosst
ISSN: 2321-2837 (Online)
ISSN: 2321-6506 (Print)
Volume 14, Issue 3, 2025
September–December
DOI (Journal): 10.37591/RRJoSST
Research RRJoSST

Seasonal Variation of VLF Radio Wave Signal Strength at 19.8s kHz Received at Khatav, India (16°46′N, 75°53′E)

C.T. More[1,*], B.R. Vibhute[1], M.C. More[2]

Abstract

This research is a detailed study of the seasonal behavior of the VLF field strength of the waves transmitted by VLF station NWC Australia (19.8 kHz). This research was carried out by using the VLF Field Strength Monitoring System located at Khatav, India (16°46′N, 75°53′E) during the period of August 2009 to July 2010. This study explores how the ionosphere and VLF radio waves react to the solar radiation. In this study, signal strength recording shows seasonal variation, which depends on the illumination of the propagation path by the sunlight. In this case, the signal strength is more stable during daytime and fluctuates during nighttime due to the presence and absence of the D-region during daytime and nighttime, respectively. Also, it is observed that the sunrise and sunset time varies seasonally throughout the whole year. It is observed that the ionosphere varies diurnally and seasonally depending on the amount of direct sunlight received at the top of the atmosphere. The height of the ionosphere is lower in summer and during the day, and electron densities are higher. With this, it was expected that SID strength might also vary by season.

Keywords: VLF, monitoring system, transmitter-receiver great circle path (TRGCP), EUMETSAT's Meteosat-9 satellite, radio wave

INTRODUCTION

The seasons on Earth have a significant impact on our lives. The seasons also affect VLF radio waves that are reflected from the ionosphere. The Field Strength of the NWC station of frequency 19.8 kHz signal and the NAA station of frequency 24 kHz recorded at Khatav, India, have been utilized to determine the seasonal behavior of the strength of VLF subionospheric waves. The propagation path of these two VLF radio stations' signals is partially over land and partially over sea [1]. The path between the Transmitter and the Receiver is more than 6 Mm.

The D-region conductivity increases exponentially as height increases. Along the propagation path, the conductivity also changes with latitude and longitude. The VLF waves travel between the ground surface and the lower ionosphere. This region, which spans the earth-ionosphere boundary, acts as a good electrical conductor. The VLF waves reflect from both these surfaces. The Earth Ionosphere Wave Guide (EIWG) offers low attenuation to VLF waves; hence, the VLF radio waves can be received all over the world. Communications with submarines immersed in the conducting sea necessitated the use of VLF waves and later ELF waves, with their comparatively large skin depths in seawater [2, 3]. A study observed the diurnal and seasonal variation of the amplitude of VLF (17.7 and 22.9 kHz) signals propagated over

***Author for Correspondence**
C.T. More
E-mail: chandrakantmore136@yahoo.co.in

[1]Assistant Professor, Department of Physics, Miraj Mahavidyalaya, Miraj, Maharashtra, India
[2]Research Scholar, Sudden Ionospheric Disturbances Monitoring Station, Khatav, Maharashtra, India

Received Date: July 30, 2025
Accepted Date: August 07, 2025
Published Date: September 08, 2025

Citation: C.T. More, B.R. Vibhute, M.C. More. Seasonal Variation of VLF Radio Wave Signal Strength at 19.8s kHz Received at Khatav, India (16°46′N, 75°53′E). Research & Reviews: Journal of Space Science & Technology. 2025; 14(3): 1–9p.

long distances (>5000 km) [4, 5]. Variations of VLF transmitter signals show amplitude minima associated with phase steps during sunrise and sunset transitions between transmitter and receiver, which could not be explained by single-mode propagation theory. It is suggested that multiple modes are needed to explain VLF propagation in the EIWG. Crombie proposed a model based on two modes being present in the nighttime portion of the propagation path and only one mode in the daytime portion of the propagation path in the EIWG [5, 6, 9].

Clivered has presented some interesting long-term studies of VLF propagation over a long-term North-South path from Cutler (USA), Marine (NAA transmitter, 24 kHz) to Faraday, Antarctica. They found the timings of the minima in the received signal strength to be remarkably consistent from year to year. They also found that the timings of minima were consistent with modal conversion taking place as the day-night boundary (terminator) crossed the propagation path, at specific, consistent locations [5, 7].

Seasonal Variation of the Field Strength of 19.8 kHz

A simple square and hexagonal loop antenna, installed at a distance of 50 ft from the receivers, has been employed in this station. The software receivers receive both the VLF transmitted frequencies. The signals captured by loop antennas are detected, amplified, rectified, and the receiver output measures signal strength in DC voltage, yielding amplitude values at the sampling rate of 5 sec. Transmitter-Receiver Great Circle Path (TRGCP) for NWC-Khatav is 6 Mm. The diurnal variation of the amplitude of the signal as recorded by the SID Monitoring System is presented. The daytime VLF signal strength is more than the nighttime VLF signal strength. This is due to the higher attenuation rate of Earth's Ionosphere Wave Guide for daytime VLF radio propagation [8]. The signal strength received depends on a number of factors such as surface conductivity, excitation of modes, path attenuation, ionosphere height, and the direction of propagation. The attenuation rate of VLF radio signals for southeast-to–west-north propagation is less than for the north-west to east-west propagation. The difference in the rate of attenuation decreases when the frequency of the waves increases [9–12]. Since D-region ionization is controlled by solar radiation, the reflection height of VLF waves that of the EIWG, at night, increases by about 10–15 km from its daytime value. If the increase in the reflection height takes place, consequently, the velocity of the phase decreases, and the signal is delayed at the receiver. The amplitude data for the selected 8 days in September 2009 are over plotted in Figure 1 to indicate the reproducibility of the amplitude values over 24 h. The variation in the VLF signal is larger during the daytime than during the nighttime. But as days are changing, the variation in curves shows a signature for seasonal variation. This seasonal variation can be significantly observed if diurnal variation data for at least one year are analyzed.

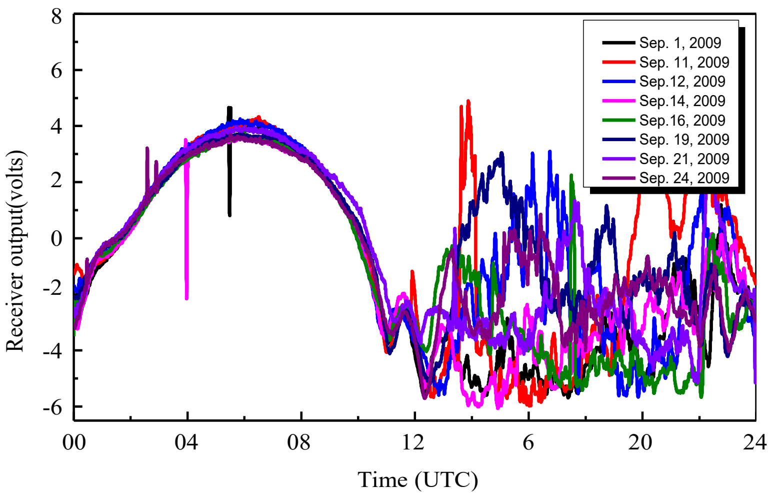

Figure 1. Diurnal variation curves for some 8 quiet days of September 2009 are over plotted. Data recorded from UTC 00.00 Hours to UTC 24.00 Hours.

As shown in Figure 1, these days are: Series 1-September 1, 2009, Series 2-September 11, 2009, Series 3-September 12, 2009, Series 4-September 14, 2009, Series 5-September 15, 2009, Series 6-September 19, 2009, Series 7-September 21, 2009, and Series 8-September 24, 2009. It is seen from the plot that there is a small variation in sunrise and sunset times for this month. All the curves show a similar diurnal pattern, but for each day, there is a very small variation in the field strength. It indicates that propagation path does not change frequently and it is more stable during the daytime. During sunrise and sunset transitions, the generation of successive minima at the receiver is observed. It is observed due to the destructive interference of propagating modes when the superposition of the waves takes place. More than two modes during the night, as well as day mode at the terminator, which is the dominant mode converted into a series of nighttime modes [13].

Seasons on Earth

The seasons of Earth are caused primarily by the tilt of Earth's rotational axis and its revolution around the Sun. These seasons are seen in Figure 2. The Earth's axis is tilted at an angle of 23.5° from the vertical. This tilt remains pointed in the same direction towards Polaris, the North Star, as Earth orbits the Sun.

Table 1 shows the times of the beginning of seasons and Earth's perihelion and aphelion. The equinox times show the beginning time of fall and spring. The solstice times show the beginning of summer and winter. Definitions of these terms can be found in The Astronomical Almanac Online glossary [14].

It is well known that Earth revolves around its axis as well as around the sun. It takes 24 h and 365 days to complete these revolutions, respectively. Earth's orbit is elliptical. The average distance between Earth and the sun is 93 million miles, and the distance varies throughout the year. In January, this distance is 1.6 million miles, which is the nearest distance to the sun. It is called the perihelion.

In July, this distance is 1.6 million miles farther away from the sun. It is called aphelion. The situation is exactly opposite in the Northern Hemisphere and the Southern Hemisphere.

Table 1. Years and dates of perihelion, aphelion, equinoxes and solstices.

Year	Perihelion	Aphelion	Equinoxes	Solstices
2009	Jan 4	July 4	Mar 20 Sep 22	June 21 Dec 21
2010	Jan 3	July 6	Mar 20 Sep 23	June 21 Dec 21
2011	Jan 3	July 4	Mar 20 Sep 23	June 21 Dec 21
2012	Jan 5	July 5	Mar 20 Sep 22	June 20 Dec 21

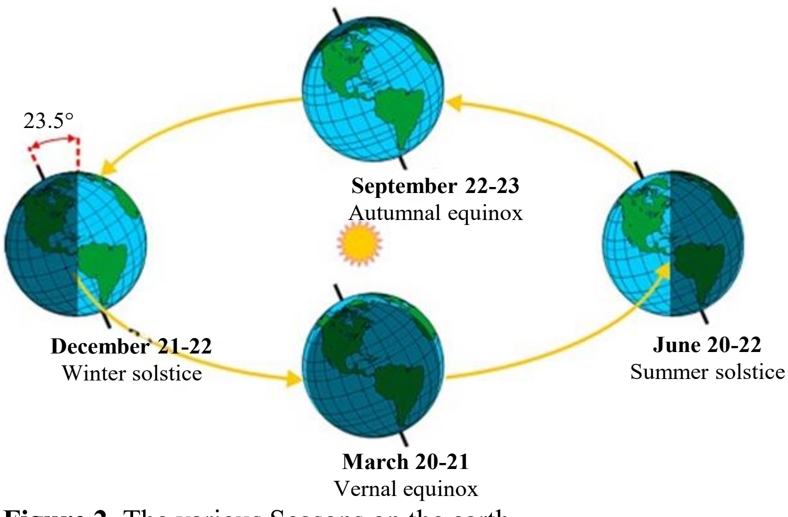

Figure 2. The various Seasons on the earth.

As we know, the Earth is tilted on its axis by 23.5°, and this is the reason behind the seasons on the Earth. The orientation of the tilt with respect to space remains constant throughout the year. As illustrated in Figure 1, the Northern Hemisphere is seen to be tilted toward the sun in the month of June and away from the sun in the month of December [15].

The Figure 3 illustrates how Earth's northern half receives more light in June, while the southern half gets more sunlight in December [15]. At the same time the Northern Hemisphere gets more solar radiation for short period of time. These views of earth from the Spinning Enhanced Visible and Infrared Imager on EUMETSAT's Meteosat-9 satellite are shown in Figure 3.

In Figure 3, the terminator line is seen on 21st December 2010 (upper left), 20th March 2011 (upper right), 21st June 2011 (lower left), and 20th September 2010 (lower right) [16].

The sequence illustrates how Earth's northern half receives more sunlight in June, while the southern half gets more light in December. When the summer begins in the Northern Hemisphere, the South Pole is tilted away from the Sun, and winter is starting in the Southern Hemisphere. The sunlight rays spread on a larger surface and travel more path in the atmosphere before reaching to earth. The reverse situation can be there in December, when the Southern Hemisphere receives most direct rays from the sun incident on the earth.

The amplitude of received VLF signals of VLF radio propagation is a useful tool for long-distance communication systems. From the observations of 19.8 kHz during August 2009 at Khatav, India (16°46' N, 75°53' E), this signal is transmitted by North West Cape, NWC Cape, North Australia (22°49' S, 114°25' E), with 1 MW radiated power. Then, as the VLF transmitter propagates mostly in the South-East direction to Khatav, the waveguide parameters can be estimated. The amplitude data recorded at 5-sec intervals have been used for analysis of VLF data.

Monthly response of VLF Field Strength

For this study, the field strength of VLF data has been collected for more than one continuous year from July 31, 2009, to August 2010, during which the solar activities were quiet minimum. Figure 4 shows seasonal variation in the field strength of VLF radio station NWC, Cape North Australia, observed at Khatav (India) for the months from August 2009 to August 2010.

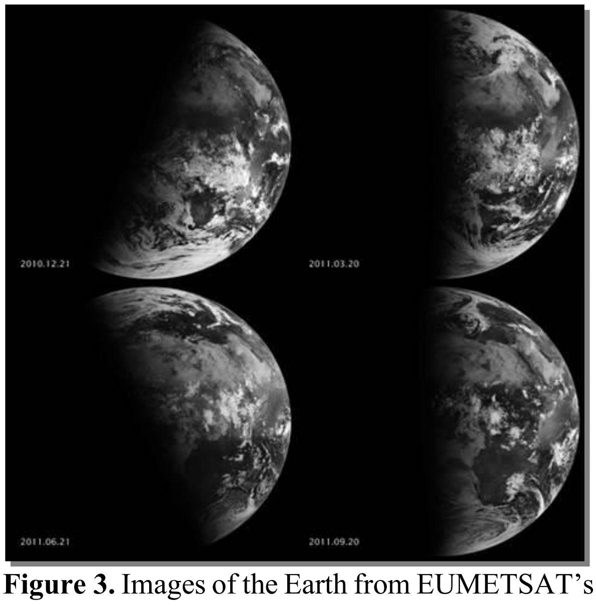

Figure 3. Images of the Earth from EUMETSAT's Meteosat-9 satellite. It shows the terminator line on September 20, 2010 (lower right), and June 21, 2011 (lower left). March 20, 2011 (upper right), and December 21, 2010 (upper left).

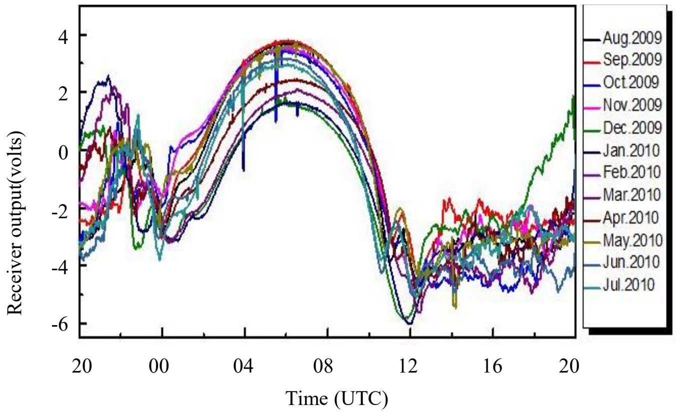

Figure 4. The Monthly average curves of diurnal variations for the period from August 2009 to July 2010 are overplotted. (Data considered for UTC 20.00 Hours of the previous day to UTC 20.00 Hours of the main day to look at the special diurnal variation shape).

Monthly Diurnal field strength variations of NWC Cape North Station, shown in Figure 4, are for various months as Series 1-August 2009, Series 2-September 2009, Series 3-October 2009, Series 4-November 2009, Series-5-December 2009, Series 6-January 2010, Series 7-February 2010, Series 8-March 2010, Series 9-May 2010, Series 10-June 2010, Series 11-July 2010. Figure 5 which shows the monthly average curves of diurnal variations for the period from August 2009 to July 2010 are overplotted. Figure 5 shows how sunrises and sunsets vary from season to season.

It is not until the ground and oceans absorb enough heat to reach equilibrium with the temperature of the atmosphere that we feel the coldest days of winter or the hottest days of summer. The recordings were not done for a few days in October 2009 and a few days in May 2010 (As the receiving system was under repair in October 2009 and the transmission from VLF station NWC Cape North was not available in May 2010). As explained earlier, one can obtain the field strength variation at the receiver input by dividing the detector output voltage by the amplification factor of the receiver. The monthly average curves of undisturbed days are superimposed in one diagram for easy comparison to bring out seasonal variation.

Table 2 shows the maximum daytime values of the detector (receiver) output voltage and field strength at the input of the SID Monitor. From Figure 5, it is observed that during the month of August 2009, the signal strength is a maximum, and during the month of January 2010, it is a minimum. Further, the field strength increases up to the month of July 2010. The signal strength variation for quite days such as July 1, July 6, July 8, July 11, July 14 of the year 2010 are used in this graph.

Figure 6 shows the graph of variation of the length of the day throughout the year during the period from August 2009 to July 2010. In Figure 7, it is observed that the length of the day increases from the month of August 2009 and reaches to maximum value in January 2010. Further, the length of the day decreases up to July 2010.

Figure 8 shows the overlapping curves of minimum signal strength at sunrise and minimum signal strength at sunset. From the graph, it is observed that when the minimum field strength at sunrise is maximum, at the same time, the minimum field strength at sunset is at its minimum level.

DISCUSSION

As is well known, waves in the VLF range propagating in the ionosphere-ground waveguide are generally very stable in amplitude during nighttime and daytime. During the sunrise and the sunset, other propagation modes can interfere with the first normally propagating mode and cause the observed fading. The transition hours, day-night and night-day, are (apart from disturbed periods) hours in which the amplitude suffers more heavy variations.

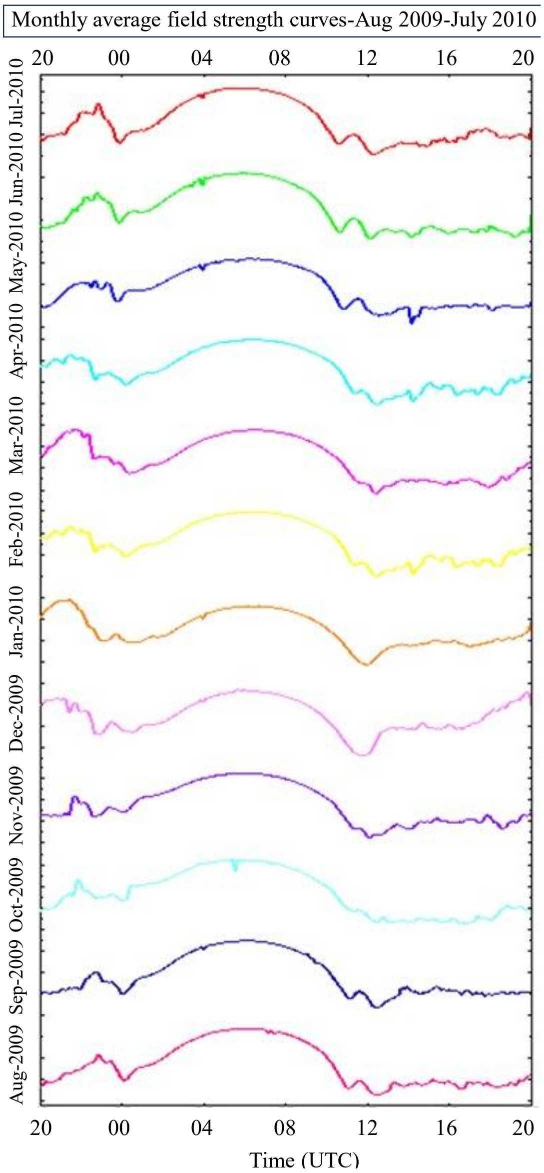

Figure 5. The Monthly average curves of diurnal variations for the period from August 2009 to July 2010 are over plotted.

Table 2. Seasonal variation of maximum daytime field strength of 19.8 kHz transmission (during the period from August 2009 to July 2010) recorded at Khatav (India).

Month/Year	**Maximum daytime detector Output (V)**	**Field strength at the Input of SID Monitor (mV)**
August 2009	10.46	1.31
September 2009	10.43	1.31
November 2009	9.92	1.24
December 2009	8.28	1.04
January 2010	8.17	1.02
February 2010	8.76	1.09
March 2010	9.20	1.15
April 2010	9.67	1.21
June 2010	9.82	1.23
July 2010	9.93	1.24

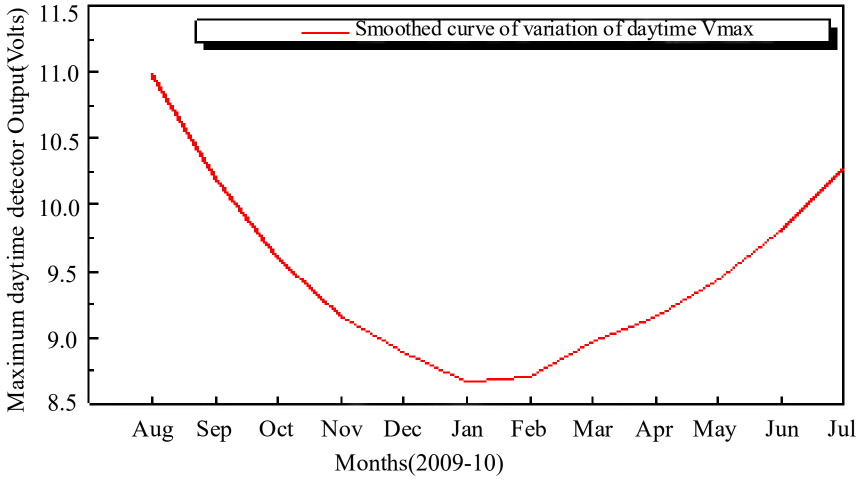

Figure 6. Smooth curve of maximum Daytime detector output (Volts).

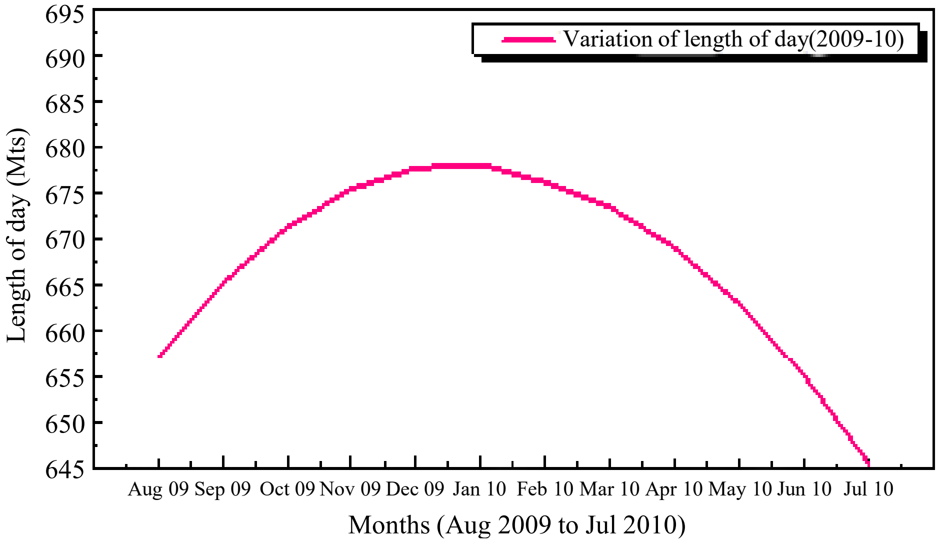

Figure 7. Smooth curve of variation of length of day (mts).

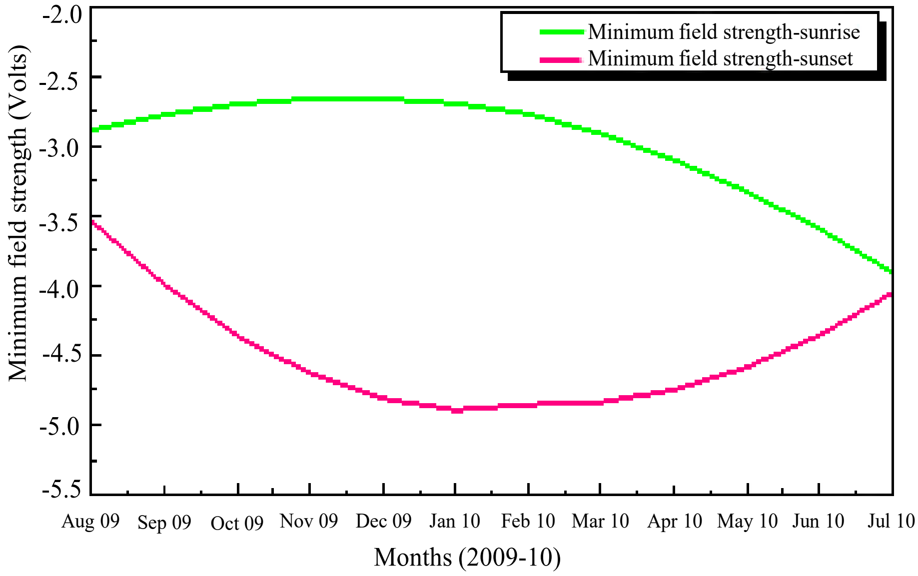

Figure 8. Smooth curves of minimum field strength sunrise and sunset measured in (Volts).

Waves with a frequency of 19.8 kHz propagate in the waveguide of height 90 km at night, 70 km in the day. The seasonal solar change is well evident for the signal coming from NWC, both for the short distance and the simple path. Data from other transmitting stations are difficult to interpret to describe low ionospheric phenomena. This kind of measurement can also be useful in disturbed days because it gives information concerning the photo-ionization of the low ionosphere during SID and other local low ionospheric events.

The peak after sunrise is probably due to the production, at dawn hours, of negative ions, followed by a rapid loss. Hours, day-night and night-day are (apart from disturbed periods) hours in which the amplitude suffers more heavy variations. Waves with a frequency of 19.8 kHz propagate in the waveguide of height 90 km at night, 70 km in the day. The seasonal solar change is more evident for the signal coming from NWC than from NAA.

CONCLUSION

This detailed study of seasonal variations during different seasons by considering the daytime modes and more modes in the nighttime will further enhance the understanding of this subject and be useful for further VLF study.

It is observed that the ionosphere varies diurnally and seasonally depending on the amount of direct sunlight received at the top of the atmosphere. The height of the ionosphere is lower in summer and during the day, and electron densities are higher. With this, it was expected that SID strength might also vary by season.

REFERENCES

1. More CT, Sharma AK, Bhonsle RV, Lynn KJ. Field strength measurement of VLF radio wave propagation at 19.8 kHz between Australia and India. In 10th Australian Space Science Conference Proceedings. 2010 Sep; 249–262.
2. Cohen MB, Inan US, Paschal EW. Sensitive broadband ELF/VLF radio reception with the AWESOME instrument. IEEE Trans Geosci Remote Sens. 2009 Sep 29; 48(1): 3–17.
3. Cummer SA, Inan US, Bell TF. Ionospheric D region remote sensing using VLF radio atmospherics. Radio Sci. 1998 Nov; 33(6): 1781–92.
4. Sulic DM, Sreckovic VA. A comparative study of measured amplitude and phase perturbations of VLF and LF radio signals induced by solar flares. arXiv preprint arXiv:1404.1019. 2014 Apr 3.
5. Clilverd MA, Thomson NR, Rodger CJ. Sunrise effects on VLF signals propagating over a long north-south path. Radio Sci. 1999 Jul; 34(4): 939–48.
6. Pal P, De BK. Studies on VLF propagation in relation to solar and geo-physical events. Conference URSI GA 2005. 2021 Nov.
7. Barr R, Jones DL, Rodger CJ. ELF and VLF radio waves. J Atmos Sol-Terr Phys. 2000 Nov 1; 62(17–18): 1689–718.
8. Šulić DM, Srećković VA, Mihajlov AA. A study of VLF signals variations associated with the changes of ionization level in the D-region in consequence of solar conditions. Adv Space Res. 2016 Feb 15; 57(4): 1029–43.
9. Crombie DD. Differences between the east-west and west-east propagation of VLF signals over long distances. J Atmos Terr Phys. 1958 Jan 1; 12(2–3): 110–7.
10. Kumar S, Kumar A, Rodger CJ. Subionospheric early VLF perturbations observed at Suva: VLF detection of red sprites in the day? J Geophys Res: Space Phys. 2008;113. doi:10.1029/2007 JA012734.
11. Chakrabarti SK, Mondal SK, Sasmal S, Pal S, Basak T, Chakrabarti S, Bhowmick D, Ray S, Maji SK, Nandi A, Yadav VK. VLF signals in summer and winter in the Indian sub-continent using multi-station campaigns. Indian J Phys. 2012 May; 86(5): 323–34.
12. Kumar S. Waveguide parameters of 19.8 kHz signal propagating over a long path. Phys Res Int. 2009; 2009(1): 216373.

ISSN: 2321-2837 (Online), ISSN: 2321-6506 (Print)

13. Kumar S, Kumar A. Diurnal variation of 19.8 kHz signal propagation over long path to Suva. The South Pacific Journal of Natural and Applied Sciences. 2007; 25(1): 67–9.
14. Crouchley J, Rahmani Z. Phase and amplitude variations of 40-kHz radio waves propagating over a 7.1-Mm path. J Atmos Terr Phys. 1973 Mar 1; 35(3): 479–95.
15. Dicks DR. Solstices, equinoxes, and the presocratics. J Hell Stud. 1966 Nov; 86: 26–40.
16. Steele J. Their equinox: Mesopotamian conceptions of solstices and equinoxes. In: Advancing Cultural Astronomy: Studies In Honour of Clive Ruggles. Cham: Springer International Publishing; 2021 Apr 9; 35–49.

